Earth and Planetary Science Letters, 49 (1980) 528–550

DISCRETE SUSPENDED PARTICLES OF BARITE AND THE BARIUM CYCLE IN THE OPEN OCEAN

F. DEHAIRS [1,*], R. CHESSELET [2] and J. JEDWAB [1]

[1] *Laboratoire de Géochimie, Université Libre de Bruxelles, 50, Avenue Roosevelt, B-1050 Brussels (Belgium)*
[2] *Centre des Faibles Radioactivités, Laboratoire mixte CEA-CNRS, 91190 Gif-sur-Yvette (France)*

Received January 5, 1979
Revised version received May 29, 1979

Barite particles are a universal component of suspended matter in the Atlantic and Pacific Oceans. This is demonstrated by scanning electron microscope and electron microprobe analyses of samples collected during the GEOSECS program. These discrete particles, about 1 μm in diameter, account for by far the greatest part of the total particulate barium of most of the filters collected at different depths. Total particulate barium (mean value: 20 ng/kg seawater) was measured on the same filters by instrumental neutron activation analysis.

Several observations indicate that biochemical, rather than purely chemical, processes are involved in the formation of the $BaSO_4$ mineral in the water column. Sr/Ba molar ratios among the individual barite grains, particularly from surface waters are extremely variable, which would not be anticipated for purely chemical interactions. Barite crystals occurring within fecal debris have been observed throughout the water column. Within such debris decomposition of the abundant organic matter may provide the micro-environment predicted as necessary for the precipitation of $BaSO_4$. Finally, a strong correlation between nutrient content and particulate barium is found in the upper 1000 m of the water column, which also suggests a control of barite formation by biota.

Some of the barite dissolves at depth in the water column. Dissolution rates were calculable for two GEOSECS stations, from which a dissolved barium flux of 0.4 $\mu g/cm^2$ yr was deduced. This figure is of the same order as the dissolved barium flux calculable from the barium content and known dissolution rates of calcareous and siliceous tests: approximately 0.5 $\mu g/cm^2$ yr. These fluxes represent the largest source of dissolved barium in the water column, the other being river input (0.6 $\mu g/cm^2$ yr). This supports the contention that the barium in the water column is mostly recycled. The residual flux of barite-Ba reaching the sea floor is of about equal importance as the flux of barium associated with fast-settling fecal material. These two sources together are almost sufficient to account for the total sedimentation rate of barium.

1. Introduction

During the past twenty years the distribution of dissolved Ba in the world ocean has been extensively studied [1,2]. The profiles of dissolved Ba are characterized by a depletion in surface water and an enrichment in deep water. This suggests a close association of Ba with the biological cycle [3,4].

An association of Ba with biogenic particles is deduced from the fact that sediments underlying highly productive surface waters are enriched in Ba [5–8] and subsequently in sedimentary barite [7]. Submarine volcanism however, may be locally important [9]. Because of the good correlation observed between dissolved barium and silicon in the water column it has been suggested that the distribution of both elements is governed by the dissolution of Ba-enriched siliceous frustules [4,10–12]. This conclusion was supported by earlier observations that some diatom species are able to accumulate significant amounts of Ba [13,14].

Other ideas have been put forward concerning the mechanism of Ba uptake by organisms and by their

* Present address: Dienst Analytische Scheikunde, Vrije Universiteit Brussel, 2 Pleinlaan, B-1050 Brussels, Belgium.

GEOSECS Publication No. 125.

detritus. A precipitation of barium sulphate in decaying, sulphate-rich organic micro-environments was proposed by Chow and Goldberg [1]. Likewise, Turekian [15] concluded that the distribution of Ba in the sediments could be explained by the production of barium sulphate crystals in association with biological activity and their partial dissolution in deep water. The involvement of barite in at least some biological processes has been confirmed by the observation of barite crystals within the protoplasm of abyssal benthic Rhizopoda of the class Xenophyophorida [16,17,45].

Previous to the first measurements of particulate barium in suspended matter samples [18] (collected during the 1972 R.V. "Jean Charcot" cruise (Harmatan expedition) in the Equatorial Atlantic and the Gulf of Guinea), no direct evidence of the presence of a barium-rich phase in suspension was available.

The data presented here were mostly obtained during the GEOSECS program [19,20]. Scanning electron microscope and electron microprobe (SEM-EMP) analyses have permitted the identification of a barium- and sulphur-rich phase in samples of suspended matter in seawater. The chemical composition and electron micro-diffractometry observations confirm the identification of these particles as barite. The mass of Ba carried by the barite particles was estimated from particle size measurements by electron microscopy and was subsequently compared with data on total particulate Ba, obtained for the same samples by instrumental neutron activation analysis (INAA). In this study we attempt to elucidate the origin of suspended barite and its importance as a source of dissolved Ba in deep water and of sedi-

TABLE 1

Geographical position of stations and investigated depth intervals

Stations	Positions	Investigated depth (interval in meters)
Atlantic Ocean		
GEOSECS station 17	74°56′N, 01°07′W	992–3439[a]
5	56°54′N, 42°47′W	363–2464 [a]
3	51°01′N, 43°01′W	28–3660 [a,b]
27	42°00′N, 41°59′W	1441–4858 [a]
31	27°00′N, 53°31′W	1–5500 [b]
58	27°02′S, 37°00′W	197–4422 [a,b]
67	44°58′S, 50°10′W	40–5580 [a,b]
91	49°36′S, 11°37′E	486–3074 [a]
82	56°15′S, 57°38′W	1–5202 [a,b]
ATLANTIS II station 715	52°56′N, 36°13′W	2000 [a]
2111	33°41′N, 57°38′W	2195 [a]
HARMATAN 1971 station 6	04°30′N, 19°35′W	2000–3000 [a]
15	00°00′ , 05°30′W	1000–4000 [a]
MIDLANTE 1974 station 50	34°43′N, 29°34′W	985–3510 [b]
Madcap	28°40′N, 25°25′W	1075–5043 [b]
TRANSAT 1975 station 17	34°06′N, 61°17′W	5–4380 [b]
Pacific Ocean		
GEOSECS station 257	10°10′S, 170°00′W	1263–5182 [a,b]
263	16°36′S, 167°05′W	676 [a]
269	23°59′S, 174°26′W	1253–6348 [a,b]
310	26°55′S, 157°11′W	1557–4789 [a,b]
282	57°35′S, 169°36′E	2131–5187 [a,b]

[a] Inspected for $BaSO_4$ presence by SEM-EMP.

[b] Analysed for total Ba_p by INAA.

mentary barite. The geographic coverage of this study can be ascertained by examining the locations of the suspended matter profiles in Table 1.

2. Methods

Specific details concerning the techniques of sampling, filtration and weighing of total suspended matter during the GEOSECS program are given in Brewer et al. [21].

2.1. Chemical analysis of particulate barium by instrumental neutron activation analysis

Quantitative analysis of particulate Ba (Ba_p) was performed by INAA, at the Centre des Faibles Radioactivités (CFR, CNRS-CEA *, Gif-sur-Yvette, France) using the facilities of the Pierre Süe Activation Analysis Laboratory (CNRS-CEA, Saclay, France).

The samples were pelletized using a specially designed stainless steel press. The standards consisted of multi-element solutions, including Ba, adsorbed on pelletized Whatman No. 41 filters. These standards, as well as blanks, were included on each irradiation run of suspended matter samples. After an irradiation of 10 min. in a neutron flux of the order of 2.3×10^{13} neutrons/cm^2 s in the EL3 reactor at Saclay Nuclear Centre, we analysed for ^{139}Ba (period: 89 minutes; ^{138}Ba (n, γ)), with a Ge-Li detector having a resolution of about 1 keV/channel.

The 2σ confidence levels mentioned in the tables and figures are determined by the counting statistics in the 166-keV photo-peak region.

2.2. Electron microscope and electron microprobe analysis

Determination of the elemental composition of barium-rich particles by SEM-EMP. The elemental composition and morphology of Ba-rich particles were studied at the Université Libre de Bruxelles (for some samples at CFR), using scanning electron microscopes equipped with electron microprobes. Both energy-dispersive spectrometers (EDS) with software facilities for X-ray data treatment, and wavelength-dispersive spectrometers (WDS) were used.

For SEM-EMP investigation, the sample consisted of a small portion (approximately 0.5 cm^2) of the original filter, mounted with colloidal carbon onto an aluminium stub and vacuum coated with carbon.

The EMP detection of Ba-rich particles was accomplished by one or the other of the following methods:

(1) By scanning the sample at constant magnification; every particle composed of high-Z elements ($Z > 13$), was checked for dominance by Ba and S with the EDS. As is well known, the EDS cannot resolve the Ti-K and the Ba-L lines. Definitive identification was based on the appearance of the general spectrum or by checking with the WDS, which resolves both lines.

(2) By a semi-automatic method which consisted of scanning several fields at a low magnification (600 X or 12,000 X) with the WDS set to diffract the Ba-L_α spectral line, while the Ba X-ray map was photographically recorded and compared with the SEM picture in order to localize the Ba containing particles. These were checked with the EDS for S content.

For both methods, if Ba and S were present as the only principal components (K, Sr are sometimes present in minor amounts), the particle was recorded as barium sulphate.

The detection limit of the EDS system is between 100 and 1000 ppm.

Confirmation of the suspended barium sulphate particles as barite. Electron micro-diffraction patterns of Ba- and S-rich particles in the GEOSECS suspended matter samples were obtained by Klossa [22]. These particles are dense and highly absorbant and proved to be extremely opaque to electrons. In order to obtain a definitive identification the use of a 1-MeV electron microscope, equipped with a goniometer stage, was required. We illustrate this work (Fig. 1) with an easily oriented single crystal, for which it was possible to identify a large number of crystal plane families, according to the degree of rotation and inclination of the stage. The results confirm that it is a highly crystalline barite particle.

* Centre des Faibles Radioactivités, Centre National de la Recherche Scientifique–Commissariat à l'Energie Atomique.

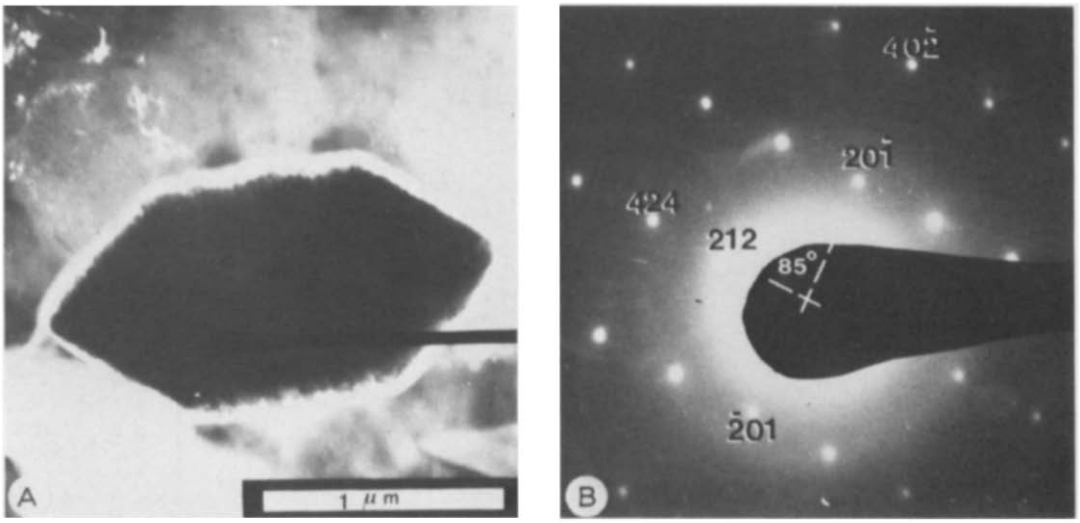

Fig. 1. Dark-field micrograph, obtained with a 1-MeV transmission electron microscope, of a single $BaSO_4$ grain, previously located on the filter by SEM-EMP (1860 m, GEOSECS station 17). Despite the penetrating power of the 1-MeV electrons only grain margins permitted any intense diffraction (A). In B one can distinguish the planes of the (212) and the $(20\bar{1})$ families, which form an angle of 85°. (From J. Klossa, Laboratoire R. Bernas, Orsay and Centre des Faibles Radioactivités, Gif-sur-Yvette.)

Estimation of the mass of barium carried by barite particles. We evaluated the contribution of the barite particles to the total particulate Ba for 12 samples from GEOSECS station 67; 8 samples from GEOSECS station 3 and 2 samples from GEOSECS station 5. To do this required that the mass of Ba carried by the barite grains be known. Particle size analysis was thus a prerequisite for the computation of particle masses. This was done by the following procedure. In order to more easily observe the sparsely scattered grains we reconcentrated the particles by resuspending the filtered matter present on 1/4 (225 mm^2) of the original Nuclepore membranes in prefiltered A.R. grade CCl_4, and re-filtered onto a much smaller Nuclepore membrane surface (37 mm^2) under a laminary flow hood. The samples were then prepared for SEM-EMP analysis as discussed above. The barite particles detected were photographed at a fixed magnification (12,000X). The images were projected on a scan table equipped with a coordinatograph. The final magnification at the scan table was 30,000X and the accuracy of the size measurements was 0.003 μm.

Only two-dimensional images are obtainable but since most of the barite particles were equant and rounded we have used the convention of projected area diameters [23] to obtain estimates of grain volumes. After inserting the projected area diameters into classes of a geometric progression a histogram of size (volume) distribution was obtained. The mass of Ba of equivalent spheres was then calculated with the following equation:

$$M = \frac{\pi}{6} \rho \left(\sum_i N_i D_i^3 \right) FV \qquad (1)$$

with M = Ba mass carried by barite particles (g/kg seawater); ρ = $BaSO_4$ density (4.5 g/cm^3); N_i = particle number in size class i (number/kg seawater); D_i = projected area diameter; = class-midpoint of class i (cm); F = molar fraction of Ba in $BaSO_4$ (0.59); and V = ratio of the unit volume of seawater (1 liter) to the volume of filtered seawater which is equivalent to the scanned filter surface.

3. Results

3.1. The concentration of particulate barium in seawater as a function of depth (INAA data)

The profiles of total particulate barium (Ba_p) measured for the Atlantic and Pacific Ocean by INAA are

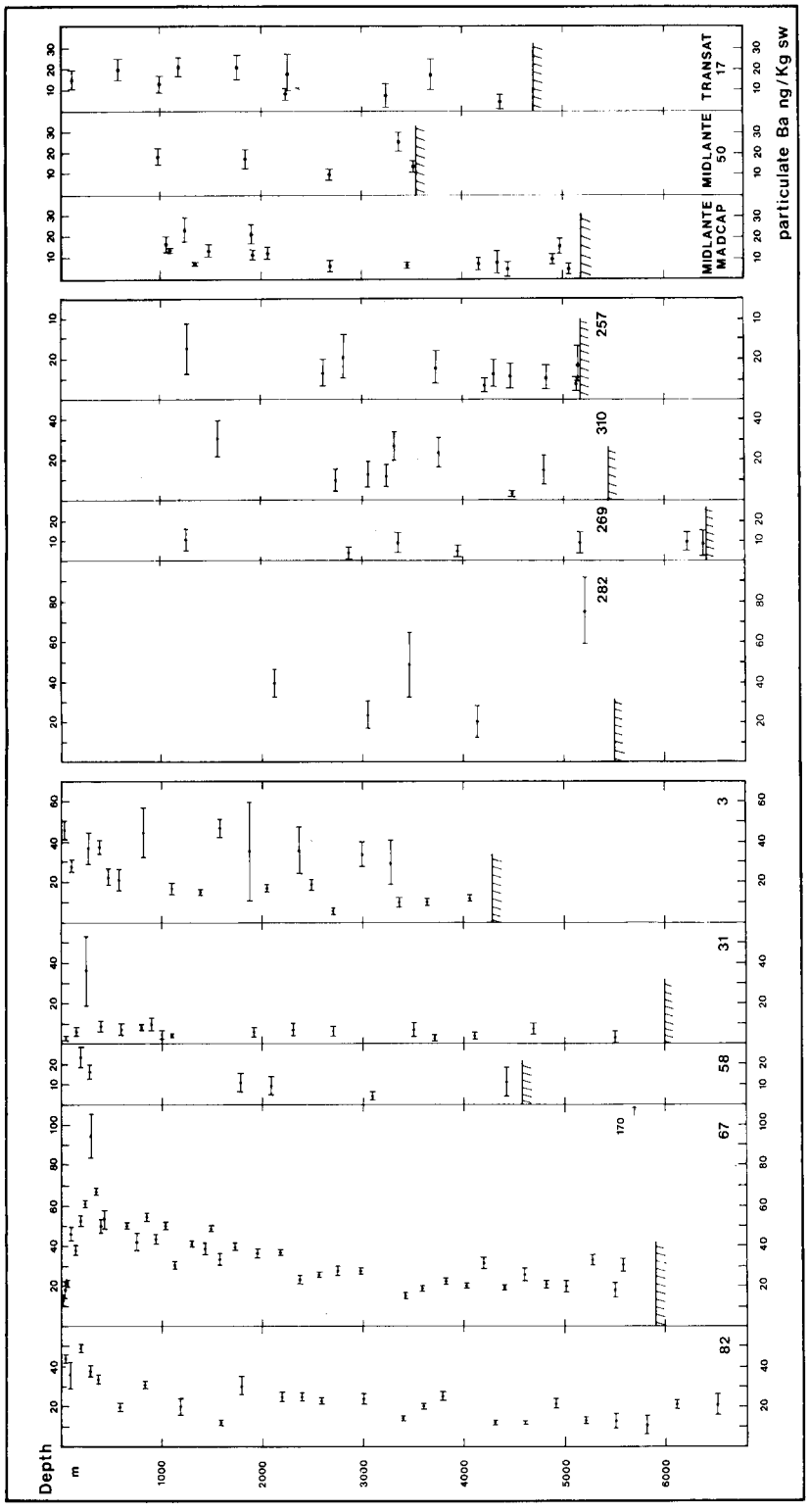

Fig. 2. Profiles of particulate Ba, measured by INAA. GEOSECS Atlantic stations 82, 67, 58, 31, 3; GEOSECS Pacific stations 282, 269, 310, 257; MIDLANTE Atlantic stations Madcap, 50; TRANSAT Atlantic station 17. For geographical locations see Table 1. The depths of the water columns are indicated by a hatched line; at station 82 this depth is 7873 m.

TABLE 2

Mean suspended barium concentration (geometric means) in surface water, in intermediate and deep water and in bottom water

Region in the water column	Stations at high latitudes: north of 45°N and south of 45°S			Stations between 45°N and 45°S		
	stations	number of investigated samples	Ba_p (ng/kg sw)	stations	number of investigated samples	Ba_p (ng/kg sw)
Surface water	GEOSECS 82, 67, 3	14	27	GEOSECS 58, 31	5	11
Intermediate and deep water	GEOSECS 82, 67, 3, 282	72	27	GEOSECS 58, 31, 310, 269, 257 MIDLANTE 50, Madcap TRANSAT 17	62	10

Region in the water column	Stations	Number of investigated samples	Ba_p (ng/kg seawater)
Bottom water [a]	GEOSECS 82, 67, 58, 31, 3, 310, 269, 257, 282 MIDLANTE 50, Madcap TRANSAT 17	28	14

[a] For the bottom waters no systematic variation of the Ba_p content with latitude is observed.

presented in Fig. 2. In order to emphasize geographic differences in the values the condensed data (geometric means) are reproduced in Table 2.

3.2. Barite in suspended matter (SEM-EMP data)

Geographical distributions. Our SEM-EMP analyses of samples collected at the stations listed in Table 1, which cover the North, Equatorial and South Atlantic, the Antarctic and the Central and South Pacific Oceans, reveal that Ba_p is almost exclusively present as discrete barite particles of about 1 μm diameter. These particles were observed in *all* investigated samples.

Elemental compositions. The suspended barite particles contain minor amounts of Sr and K. In the surface waters a broad range of Sr/Ba ratios exist. A semi-quantitative SEM-EMP study of 100 Ba-, Sr- and S-rich particles, collected in the surface water (200 m) at GEOSECS station 58, revealed that for 67% of the particles the strontium sulphate fraction, N_{SrSO_4} (with $N_{SrSO_4} + N_{BaSO_4} = 1$), was $\leqslant 0.1$; for 22% N_{SrSO_4} was between 0.1 and 0.5 and for 11% N_{SrSO_4} was >0.5 (P. Buat-Menard and C. Jehanno, personal communication; see Figs. 3, 4 and 5C). Ba-free, Sr- and S-rich particles are also present, either as biogenic debris (*Acantharia* debris; Fig. 5A, B), or as smaller particles with no obvious biogenic morphology (Fig. 5D).

Morphology. The most frequently observed morphologies for barite particles are, in decreasing order of frequencies (see Fig. 6):

– Ellipsoïdal or spherical particles.

– Particles with a distinct crystalline habit (euhedral, automorphic particles).

– Irregularly shaped particles that were probably affected by dissolution.

– Aggregates of very small particles (sub-micron sized) with or without a crystalline habit.

3.3. Non-barite particles containing barium (SEM-EMP data)

Particles with Ba as a minor constituent also occur. These particles measure between a few microns to

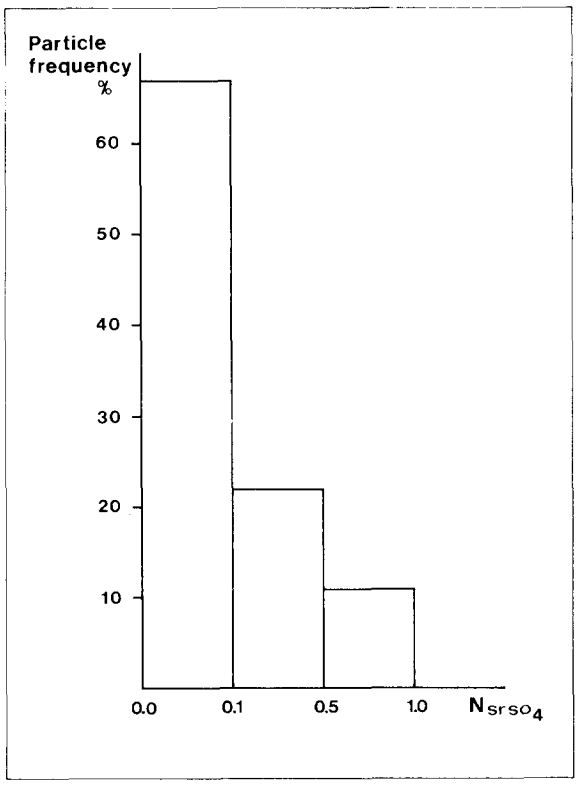

Fig. 3. Frequency histograms of (Ba, Sr)SO_4 and (Sr, Ba)SO_4 particles as a function of their $SrSO_4$ fraction (N_{SrSO_4}), for the sample from 200 m, GEOSECS station 58. We take $N_{SrSO_4} + N_{BaSO_4} = 1$. Data obtained by P. Buat-Menard and C. Jehanno at the Centre des Faibles Radioactivités, Gif-sur-Yvette.

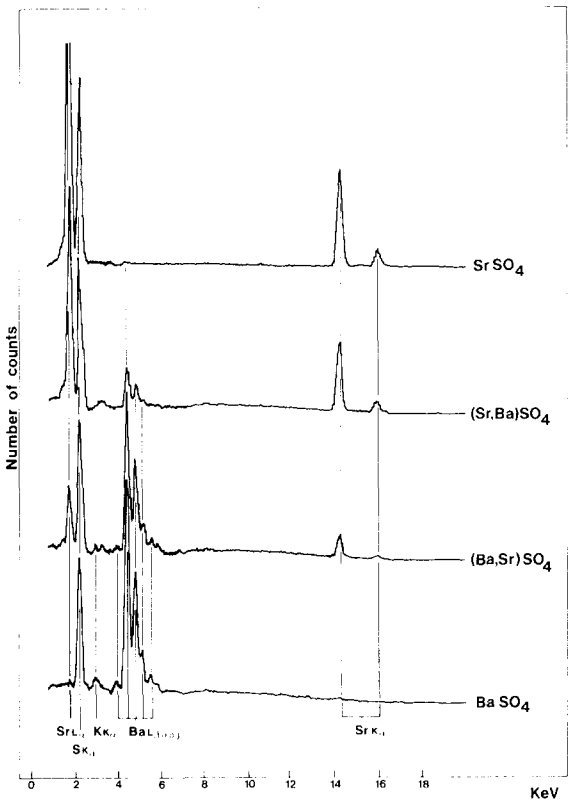

Fig. 4. Energy-dispersive spectra of barite, celestite and intermediate solid solutions, as observed in oceanic suspended matter samples. Vertical scales are arithmetic, but are normalized for the S-K_α peak which represents 58,000 counts. Horizontal scale: energies of the X-rays in keV.

several tens of microns. Two categories of such Ba-containing particles are distinguishable, based upon the nature of their principal elements:

– Particles with Fe as the major constituent. Si, Ca, Al and occasionally S, Cl are detected. Discrete Fe-rich particles in suspended matter occur mainly as goethite [24]. Scavenging of smaller particles and/or adsorption of soluble species could explain the presence of Ba and S in these particles.

– Particles with Si-Al as the major constituents. Fe, Ca, Na are occasionally detected. Harmotome, a zeolite reported to occur in the marine environment [25], seems a likely candidate. Depending on their composition (Si + Al + Na + Ba or Si + Al + Ca + Ba) other particles could represent feldspars. Adsorption processes could explain the presence of the sulphur that is occasionally detected.

3.4. The size distribution of the barite particles and associated mass of barium (SEM-EMP data)

According to the method described earlier (p. 531), the barite particle frequency, as a function of particle diameter, and the associated mass of Ba was computed for the samples listed in Table 3. The samples were randomly chosen from one profile in the Argentine Basin (GEOSECS station 67) and two profiles in the North American Basin (GEOSECS station 3 and 5). The barite particle size distributions (e.g., Fig. 7, GEOSECS station 67) are log-normal. This type of

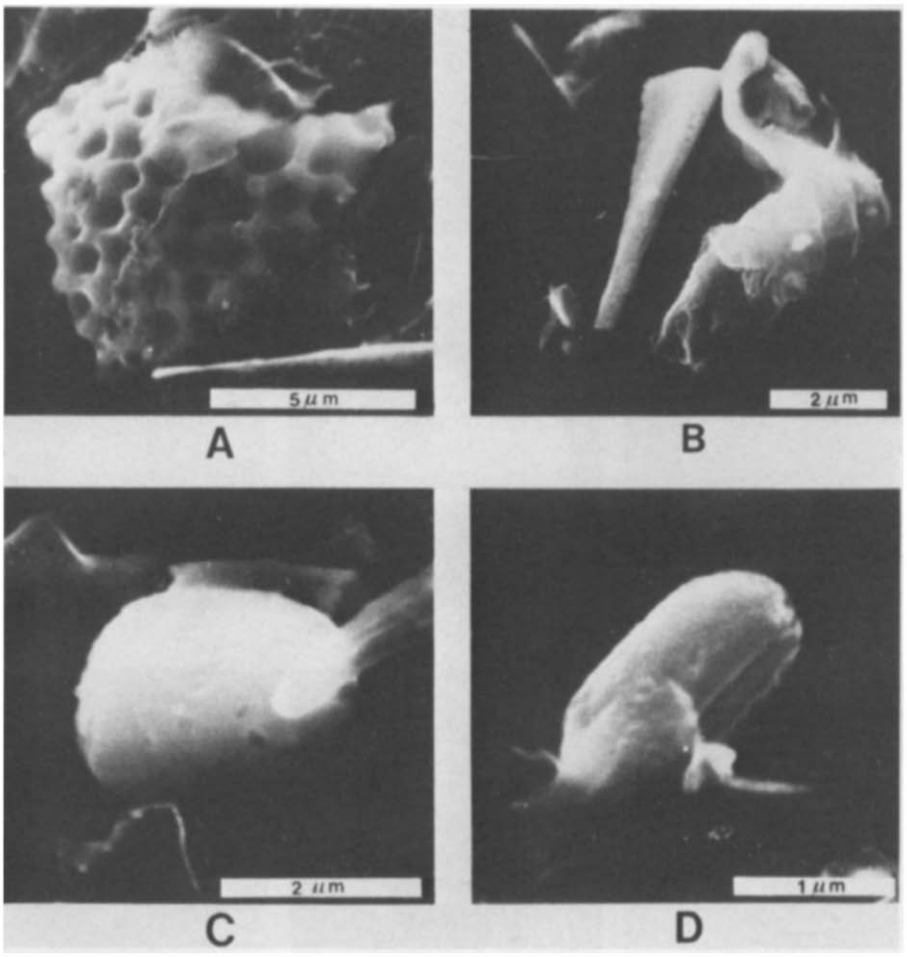

Fig. 5. Strontium sulphate and barium-enriched strontium sulphate particles. A. Biogenic SrO_4 debris: GEOSECS station 67: 151 m; elemental spectrum by SEM-EMP in Fig. 4, "SrO_4". B. Broken $SrSO_4$ spicule: GEOSECS station 67: 62 m; elemental spectrum by SEM-EMP in Fig. 4, "$SrSO_4$". C. Rounded, ellipsoidal (Sr, Ba)SO_4 particle with traces of corrosion: GEOSECS station 67: 151 m; elemental spectrum by SEM-EMP in Fig. 4, "(Sr, Ba)SO_4". D. Euhedral, slightly corroded $SrSO_4$ particle: GEOSECS station 67: 1499 m; elemental spectrum by SEM-EMP in Fig. 4, "$SrSO_4$".

distribution is not unusual and has been observed by SEM-EMP in our laboratories for other categories of suspended particles including aluminosilicates [60] and calcareous and siliceous debris [28,60]. These size distributions enabled us to compute the mass of Ba carried by suspended barite.

The computed masses of Ba are given in Table 3, column B, and are compared with INAA data on total Ba_p (Table 3, column C).

4. Discussion

4.1. Barite as a genuine component of oceanic suspended matter

The possibility of contamination by Ba-rich particles during the sampling (i.e., contamination with *exogenic* particles) and the possibility of $BaSO_4$ precipitation due to physical and chemical processes

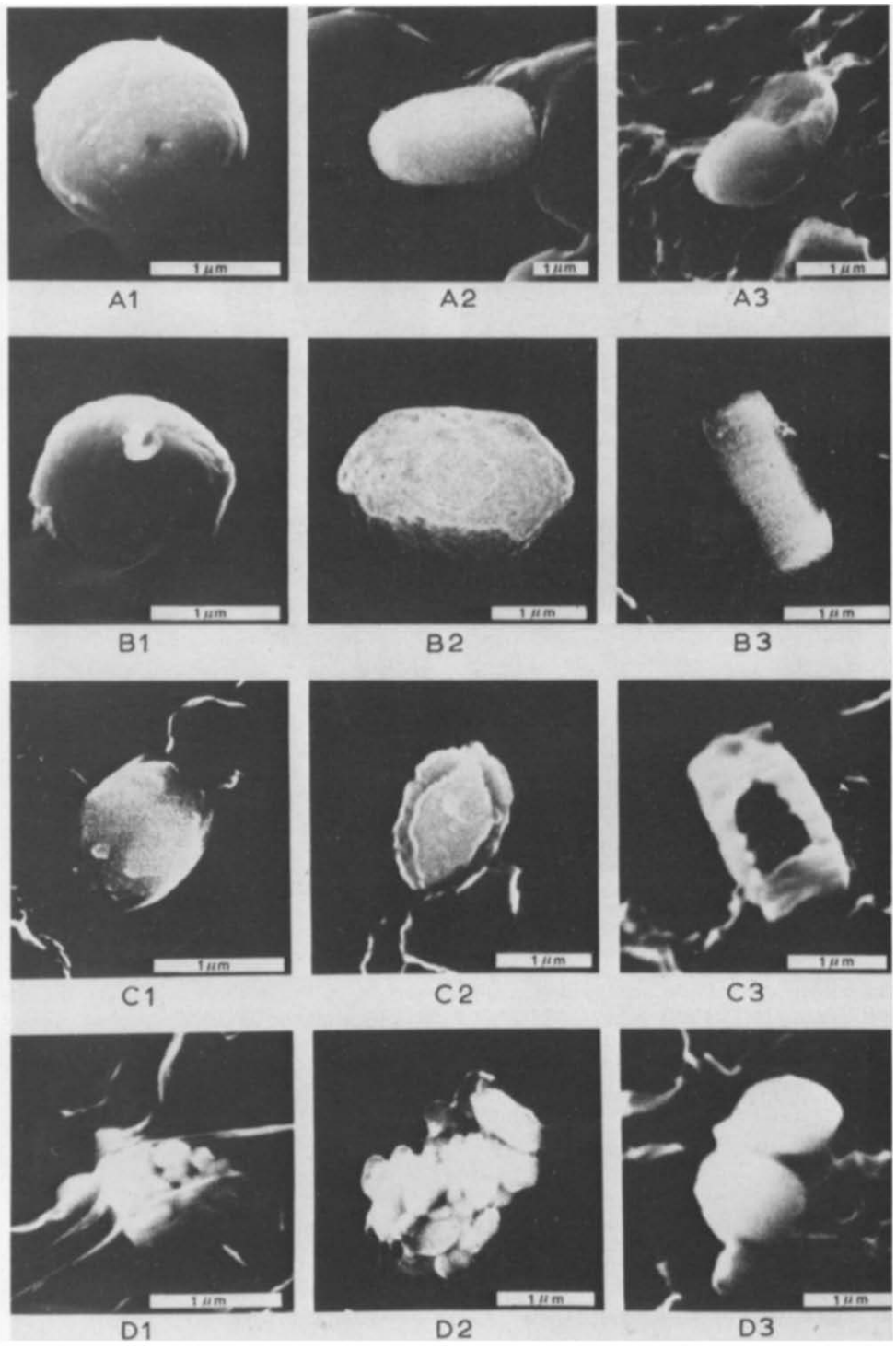

Fig. 6. Morphological types of barite particles in suspension in seawater. A. Ellipsoidal or spherical particles. 1 = GEOSECS station 67, 1499 m; 2 = GEOSECS station 3, 28 m; 3 = GEOSECS station 82, 832 m. B. Particles with a crystalline habit: euhedral, automorphic particles. 1, 2 and 3 = GEOSECS station 67, 658 m, 2982 m, and 2982 m, respectively. C. Irregularly shaped particles; probably affected by dissolution. 1, 2 and 3 = GEOSECS station 67, 2982 m, 2193 m, and 5599 m, respectively. D. Aggregates of very small particles, with or without a crystalline habit. 1, 2 = GEOSECS station 67, 62 m and 4424 m; 3 = GEOSECS station 3, 105 m.

TABLE 3

Comparison between the amount of particulate barium carried by barite particles, measured by SEM-EMP, and the total particulate barium measured by INAA

Depth (m)	A Number of barites		B Particulate Ba in barites		C Total Ba_p (INAA data)		D Fraction of total Ba_p carried by barite (%)
	(*N*/kg sw)	σ [a]	(ng/kg sw)	σ [b] (%)	(ng/kg sw)	2σ [c] (%)	
GEOSECS station 67							
151	10,600	1550	10	45	38.5	9	25
353	20,400	1960	48	54	66.9	4	72
658	16,580	1670	27	50	50.5	7	53
1053	17,820	1760	38	37	50.0	6	76
1499	12,240	1280	31	44	48.2	5	64
2193	5440	670	37	44	37.7	4	100
2574	7160	970	27	51	25.6	5	100
2982	4180	600	23	78	28.2	5	82
3601	5660	1030	15	59	19.2	9	79
4424	3440	490	15	41	19.4	9	75
5304	8820	1260	25	67	33.0	13	76
GEOSECS station 3							
105	5830	580	17	39	27.8	9	61
813	3900	390	18	53	44.2	28	41
1083	4480	630	14	59	16.9	17	83
1875	25,000	2550	31	36	35.1	70	88
2479	3930	410	15	48	18.6	14	81
2696	1970	300	5	47	5.4	19	93
2989	24,850	2740	33	54	33.6	17	98
3267	2920	470	15	87	29.5	19	51
GEOSECS station 5 [d]							
363	16,040	1830	27	47	36		75
760	46,990	5070	48	40	50		96

[a] $\sigma = 1/\sqrt{N}$, with N = number of effectively counted barites [23].

[b] $\sigma = \Sigma\sigma_i$; $\sigma_i = M_i/\sqrt{n_i}$, with M_i = % by weight in a given size range; n_i = number of particles counted in this size range [23].

[c] σ is determined by the counting statistics in the 166-keV photo-peak region.

[d] Total Ba_p data for the samples we analyzed for barite content by SEM-EMP were not available; we deduced total Ba_p values by interpolation of the data of P. Brewer (GEOSECS shore-based data), for depths immediately above and below depths investigated by SEM-EMP.

inherent in the sampling procedure (i.e., contamination with *endogenic* particles) have been considered and rejected as significant problems. This is based on the following arguments:

Exogenic origin: (1) On board ship, blanks were run under the same technical conditions as the samples. They never show contamination by Ba-rich particles.

(2) Barite particles were observed in *all* samples collected during various expeditions by different research vessels since 1972. All these samples contain the same morphological types of barite particles. This is incompatible with occurrences of accidental contamination. Furthermore, the use of different equipment for sample collection and handling during GEOSECS, ATLANTIS II, HARMATAN, MIDLANTE and TRANSAT expeditions makes a systematic contamination of the samples unlikely.

(3) On several occasions we observed barite crystals inside low-density pellet-like particles, probably

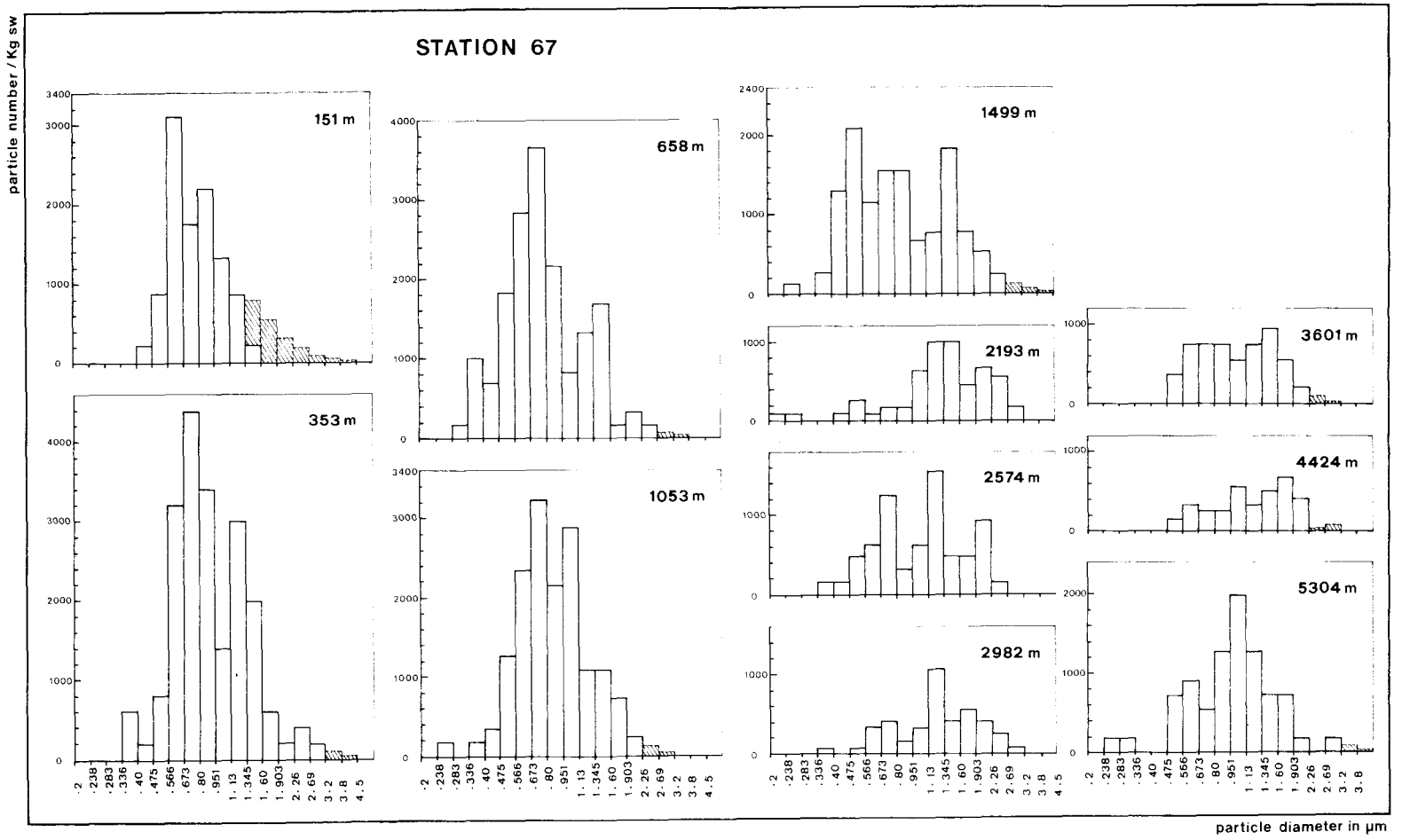

Fig. 7. Number frequency versus size of barite particles from various depths at GEOSECS station 67. For the abscissa sizes are classed in a logarithmic progression: 0.2, $0.2\sqrt[4]{2}$, $0.24\sqrt[4]{2}$, $0.28\sqrt[4]{2}$, $0.34\sqrt[4]{2}$, ... Particles smaller than 0.2 μm were not observable. The hatched areas on the right side of the histograms represent non-recorded particles, whose presence is required in order for barite to account for the total Ba_p mass. The frequencies under the hatched areas were deduced from the cumulative Ba mass distributions in Fig. 9.

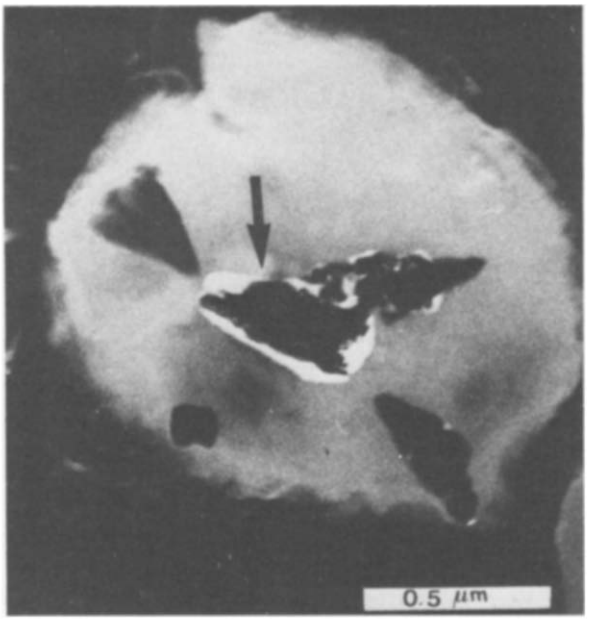

Fig. 8. Dark-field micrograph obtained with a 1-MeV transmission electron microscope of a barite grain (indicated by the arrow) inside an organic pellet, collected at 1860 m at GEOSECS Pacific station 306. (From J. Klossa, Laboratoire R. Bernas, Orsay and Centre des Faibles Radioactivités, Gif-sur-Yvette.)

of organic composition (Fig. 8). Barite particles were also found in large aggregates containing different species of diatoms and coccoliths. These pellets and aggregates represent fragments of the kinds of fecal material described by Bishop et al. [26]. These barite particles were either scavenged by zooplankton and excreted together with the fecal matter, or were formed inside such pellets. An exogenic origin can be excluded in both cases.

Endogenic origin. Several processes can induce a precipitation of barium sulphate during sample recovery:

(1) Deep-sea water samples are enriched in dissolved Ba and may approach, and eventually reach, saturation when hauled to the surface, since the effects of decompression and temperature transition decrease the saturated Ba level by a factor two [27]. However, according to Church and Wolgemuth [27] such a precipitation process, especially in heterogenous systems with a large sulphate excess, should take days. Even for the deep-sea samples, recovery time is only a matter of hours. Since deep-sea water Ba concentrations are in fact much lower than the sediment pore waters discussed by Church and Wolgemuth [27], we conclude that barite precipitation does not take place during sample recovery. In fact, barite particles were observed in samples of suspended matter which were filtered in situ, at depths of 2000 m (ATLANTIS II, station 2111) and 2195 m (ATLANTIS II, station 715) with an especially designed titanium bottle of the Woods Hole Oceanographical Institution. This technique effectively precludes barite precipitation during sampling.

(2) A possible source of endogenic contamination might be incomplete rinsing of seawater from the filters. The subsequent dessication of such microdrops of seawater can introduce contamination such as precipitated gypsum ($CaSO_4 \cdot 2\,H_2O$) [28]. The complete dessication of about 10 μl of seawater is required to obtain the weights of endogenic gypsum, measured by Aubey [28]. If we use this figure (10 μl) as a reasonable estimate of endogenic sources the maximum amount of Ba contamination from this mechanism would be 10^{-4} μg/filter. This is 1700 times less than the mean total Ba_p concentration, which consists mainly of barite (section 4.2).

We conclude from the set of arguments presented above that the barite particles we observe are a genuine component of the natural marine environment.

4.2. Is barite the main carrier of barium in oceanic suspended matter?

Table 3 compares the calculated mass of barite-Ba (column B) with the total Ba_p measured by INAA on the same filters (column C), expressed as a percentage (column D). The conclusion that barite is the principal carrier of barium in these samples is inescapable considering the nature and limitations of the method. In 15 cases out of 22, calculated barite contributions account for over 70% of the total Ba_p and for several samples the values are virtually 100%. There are only a couple of cases where the percentage drops below 50%. Part of the Ba amount that is not accounted for by detected barites is certainly carried by phases other than barite (see below). We believe that larger barite grains, which are very scarce and thus

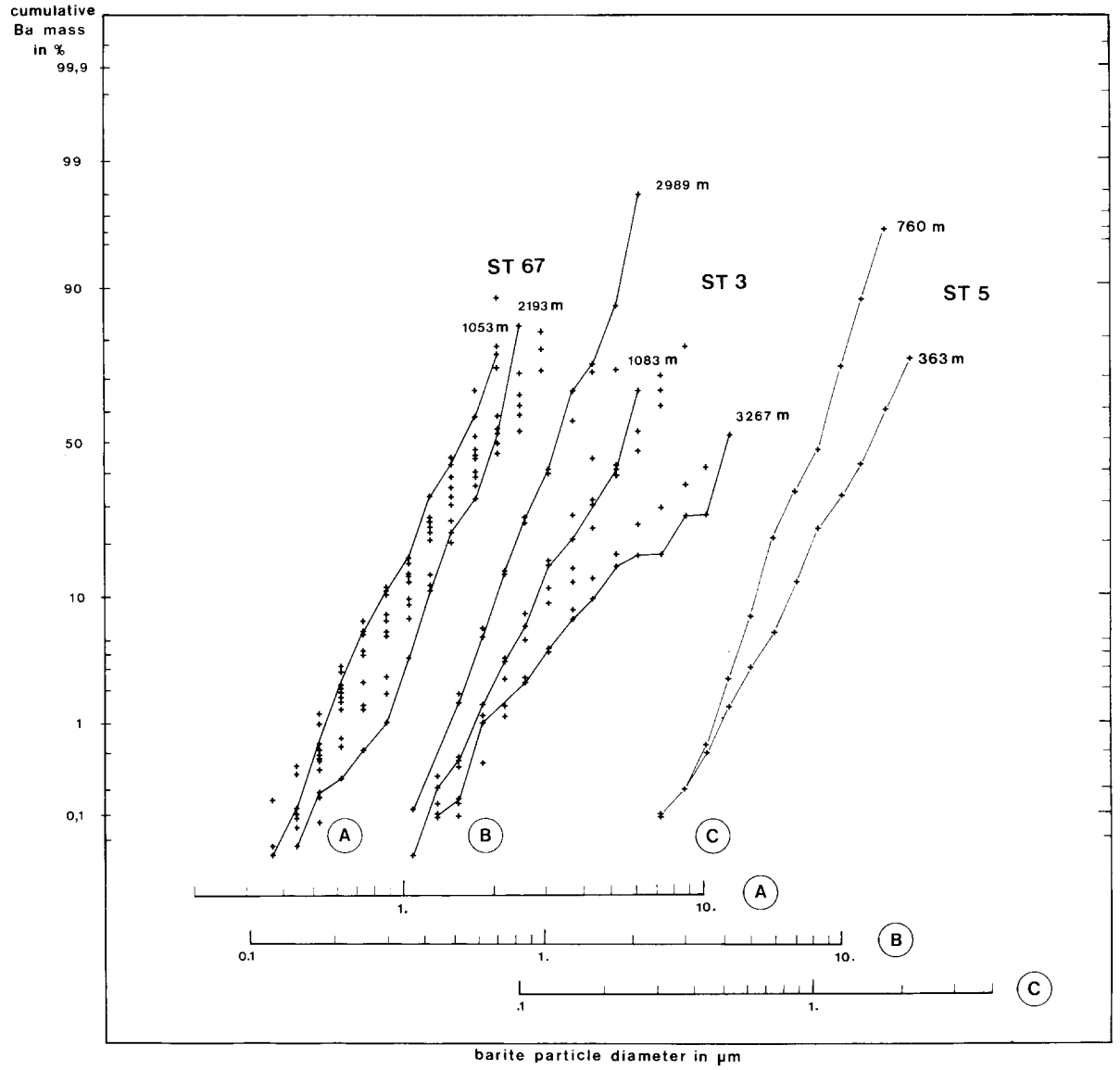

Fig. 9. Profiles of cumulative Ba mass distributions. Ordinate (gaussian scale): cumulative Ba mass in percent, calculated with respect to the total Ba_p amount measured by INAA. Abscissa (logarithmic scale: barite particle diameter in microns). Crosses correspond to measured values of cumulated Ba mass (in %). A = GEOSECS station.67; depth interval 151–5304 m; only the distributions at 1053 m and 2193 m are displayed as a solid line. B. GEOSECS station 3; depth interval 105–3267 m; only the distributions at 1083 m, 2989 m and 3267 m are displayed as a solid line. C. GEOSECS station 5; depth interval 363–760 m; both distributions are displayed as a solid line.

statistically missed during counting procedures, but which have large mass, can account partly for the apparently low percentages in Table 3, column D. In Fig. 7 we show the projected shape of the tails of the histograms if the cumulative curves of Fig. 9 are extrapolated to 100%. These tails represent the number of large barite grains, which would be required to completely account for the INAA Ba_p values, if the

other sources of particulate Ba are ignored.

The percentage Ba_p as barite figures are subject to error due to the limitations of the counting, volume estimate and mass extrapolation procedures. There are other carriers of barium in oceanic suspended matter. As discussed in section 4.3, these may account for as little as 8.5% of the total Ba_p in intermediate and deep water and as much as 50% when considering the contributions within the surface waters (first 150 m). Within the great bulk of the oceanic water column, however, it is barite which is the dominant carrier of Ba_p.

4.3. The contribution of non-barite barium carriers to total particulate barium

The role of diatom skeletons. Several authors [4,10–12], citing the correlation between dissolved Ba and dissolved SiO_2 in the water column and the work of Vinogradova and Koval'skiy [14], have suggested that diatoms play a major role in the transport of Ba. Very few experimental data exist, however, on the uptake of Ba by diatoms. We have studied this uptake in two diatom species: *Rhizosolenia alata* and *Chaetoceros lauderi.* Details concerning the experimental techniques are published elsewhere [29]. The data show that, for *C. lauderi,* Ba uptake does not exceed the INAA detection limit (~1 ppm for these series of analyses). For *R. alata* Ba is observed to be entirely associated with the silica phase obtained after oxidation of the organic fraction with concentrated peroxide. The Ba uptake is positively related to the Ba content of the growth medium (Table 4).

These Ba values are 10–100 times smaller, when compared on a whole dry matter basis, than those reported for different *Chaetoceros* and *Rhizosolenia* species from the Black Sea by Vinogradova and Koval'skiy [14]. Our data do, however, agree well with those of Martin and Knauer [31] for natural, composite diatom-rich phytoplankton, as well as with the data of Riley and Roth [32] for other cultured diatoms.

The SEM-EMP analyses performed on the diatom frustules in GEOSECS samples show that these frustules contain no Ba above the detection limit (100–1000 ppm). Therefore we will take the Ba content observed for *R. alata* frustules (120 ppm; Table 4), as a representative value for diatom frustules in the ocean.

We use the figure of 10% as the proportion of biogenic silica in total suspended matter (TSM) ([26,31, 33,34]; see Table 5, column B), to calculate the contribution of Ba from this component in Table 6, column B.

The role of carbonate skeletons. Biogenic $CaCO_3$ is assumed to contain 200 ppm of Ba [7], although this is probably an upper limit, since lower values (10–30

TABLE 4

Barium content (in ppm) of diatoms grown in culture

Diatom species	Media not enriched in Ba		Media enriched in Ba
	natural seawater; dissolved Ba content: 10 μg/kg sw [a]	artificial seawater [b]	artificial seawater; dissolved Ba content: 30 μg/kg sw [c]
Rhizosolenia alata	58 [d] 116 [e]	69 [d] 138 [e]	196 [d] 392 [e]
Chaetoceros lauderi	<1 [f]	<1 [f]	<1 [f]

[a] This value corresponds to the Ba content measured for Mediterranean Sea surface water [30], which is the natural medium in which the diatoms were grown.

[b] Ba was introduced into the culture medium as impurities in the constituents used.

[c] Ba was added as the chloride salt in order to reach a final concentration of 30 μg/kg seawater.

[d] In ppm of whole dry matter.

[e] In ppm of SiO_2 weight; for *R. alata* the SiO_2 weight represents 50% of the whole dry matter weight. Ba is entirely associated with the silica fraction.

[f] Concentrations did not exceed the detection limit (1 ppm).

TABLE 5

Concentrations of total suspended matter (TSM), siliceous and calcareous matter, particulate organic matter and aluminosilicates as potential barium carriers in the water column

Section of the water column	A TSM in the Atlantic [a] (μg/kg sw)	B SiO_2 (μg/kg sw)	C $CaCO_3$ (μg/kg sw)	D POM (μg/kg sw)	E Alumino-silicates [e] (μg/kg sw)
Surface water		(= 10% of TSM [b])	(= 6% of TSM [c])	(= 60% of TSM [d])	
high latitudes	max: 200	max: 20	max: 12	max: 120	} 2.2
low latitudes (between 45°N and 45°S)	max: 50	max: 5	max: 2	max: 30	
Intermediate and deep water (high and low latitudes)	max: 25	(= 10% of TSM [b]) max: 2.5	(= 6% of TSM [c]) max: 1.5	(= 60% of TSM [d]) max: 15	1.4
Bottom water (nepheloid layer)	range: 12–100	2.5 [f]	1.5 [f]	15 [f]	4.5

[a] From Brewer et al. [21].
[b] From Bishop et al. [26], Martin and Knauer [31], Copin-Montegut and Copin-Montegut [33,34].
[c] From Aubey [28] and CFR-GEOSECS shore-based data.
[d] From Bishop et al. [26], Copin-Montegut and Copin-Montegut [33,34], Krishnaswami et al. [35].
[e] From Al_p geometric means in Buat-Menard and Chesselet [37] and CFR-GEOSECS shore-based data.
[f] The $CaCO_3$ concentration in bottom water is similar to that in intermediate and deep water (CFR-GEOSECS shore-based data); this is assumed also for SiO_2 and POM.

TABLE 6

Contribution of siliceous and calcareous tests, POM and aluminosilicates to the total barium content of suspended matter

Section of the water column	A Total Ba_p [a] (ng/kg sw)	B Ba carried by SiO_2 tests [b]		C Ba carried by $CaCO_3$ tests [c]		D Ba carried by POM [d]		E Ba carried by aluminosilicates [e]		F Fraction of total Ba_p carried by non-barite phases (%)
		(ng/kg sw)	% of Ba_p total	(ng/kg sw)	% of Ba_p total	(ng/kg sw)	% of Ba_p total	(ng/kg sw)	% of Ba_p total	
Surface water										
high latitudes	27	2.4	9	2.4	9	7.2	27	} 1.3	5	50
low latitudes (between 45°N and 45°S)	11	0.6	5.5	0.6	5.5	1.8	16.5		12	39.5
Intermediate and deep water										
high latitudes	27	} 0.3	1	} 0.3	1	} 0.9	3.5	} 0.8	3	8.5
low latitudes (between 45°N and 45°S)	10		3		3		9		8	23
Bottom water (nepheloid layer)	14	0.3	2	0.3	2	0.9	6.5	2.7	19	29.5

[a] From Table 2.
[b] SiO_2 tests contain 120 ppm of Ba; this study (Table 4).
[c] $CaCO_3$ tests contain a maximum of 200 ppm Ba; from Church [7].
[d] POM contains 60 ppm of Ba; from Martin and Knauer [31], Riley and Roth [32].
[e] Aluminosilicates contain 600 ppm of Ba; from Turekian [15] and Turekian and Wedepohl [38].

ppm) are reported [6] for coccolith oozes. The weight fraction of biogenic $CaCO_3$ in TSM is given in Table 5, column C and the contribution of $CaCO_3$ skeletons to the total Ba_p content is shown in Table 6, column C.

The role of particulate organic matter. Particulate organic matter (POM) represents the main fraction of TSM (Table 5, column D). To estimate the Ba content of this material we have used the data of Riley and Roth [32] and Martin and Knauer [31] for skeleton-free plankton. A mean value of 60 μg Ba/g dry matter was used to calculate the POM contribution to total Ba_p in Table 6, column D.

The role of aluminosilicates. SEM-EMP and INAA analyses of GEOSECS suspended matter samples, revealed that Al can be used as an indicator of aluminosilicates in suspended matter [24,36,37] and confirm estimations of Arrhenius [25] that particulate Al represents 7–9% by weight of the total inorganic component of TSM. This quantity is equal to the Al content of shales: 8% by weight [38]. We will therefore consider the Ba concentration in shales (600 ppm [38,15]) to be representative of the Ba content of aluminosilicates suspended in seawater. The aluminosilicate content of seawater is given in Table 5, column E and the fraction of total Ba_p, carried by aluminosilicates is given in Table 6, column E.

An examination of the data in Table 6, column F shows that for the largest part of the water column (intermediate and deep water) non-barite phases account for only 8.5–23% of the total Ba_p. In surface water up to 50% of total Ba is carried by phases other than barite. Here skeletal and organic debris are important contributors to the total Ba_p content of suspended matter. In the bottom nepheloid layer non-barite phases account for 29.5% of the total. Here 19% of total Ba_p is due to aluminosilicates, most probably resuspended from the sediments in the nepheloid layer [61]. We do not have quantitative measurements for surface and bottom waters, but the remaining fraction of total Ba_p is most likely comprised of barite particles, which were indeed observed.

4.4. Origin of the barite particles

The possibility of direct precipitation of barite in seawater is presently a subject for debate. Seawater is undersaturated with respect to $BaSO_4$ but Hanor [39] has predicted that Sr-enriched barite is less soluble than pure $BaSO_4$ and might precipitate in the sea. Church [7] has shown that this concept cannot be confirmed experimentally. A lack of data on the solid activity coefficients of non-dilute (Ba, Sr)SO_4 solid solutions prevents the definitive resolution of this problem ([40], and T.M. Church, personal communication, 1979).

Our data lead us to believe that direct precipitation is not a significant process. The highly variable Sr/Ba ratios we observe among the barite particles (section 3.2) is inconsistent with authigenic formation of such variable particles in a single parcel of seawater considered as a given physico-chemical environment. In any case we observe Sr-free barites. There is no disagreement between these authors [7,39] concerning the impossibility of inorganic precipitation of barium sulphate under natural oceanic conditions.

Biological activity appears to provide the necessary intermediary for the formation of barite in seawater.

Fig. 10 shows a plot of the mean Ba_p content versus the mean dissolved PO_4 content for a broadly spaced set of stations from the Atlantic Ocean. Since Ba_p maxima occur at variable depths below the euphotic zone (Fig. 2), all concentrations from 150 m down to 1000 m were considered to compute geometric mean values. PO_4 values are from GEOSECS ship-board data and the Ba_p data for GEOSECS stations 27, 5, 11, 18 in the North Atlantic and for GEOSECS station 17 in the Norwegian Sea, are from P. Brewer (GEOSECS shore-based data). A linear relationship between Ba_p and dissolved PO_4 is apparent when considering stations 31, 58, 27, 17, 3, 5 and 67. PO_4 contents in surface waters are generally regarded as indicators of potential productivity [41–44] and these results indicate a positive relationship between Ba_p production and organic productivity. Unfortunately, direct measurements of organic carbon production were not obtained at the same time as the collection of samples for Ba and PO_4. Carbon production data taken at a different period but for the same general vicinity as these stations [41,44] are included in parentheses in Fig. 10. These data confirm the general correlation of Ba_p with biological productivity. The stations 11, 18, 23 from the Norwegian Sea and the North Atlantic, and station 82, from the Antarctic, fall much closer to the central line when

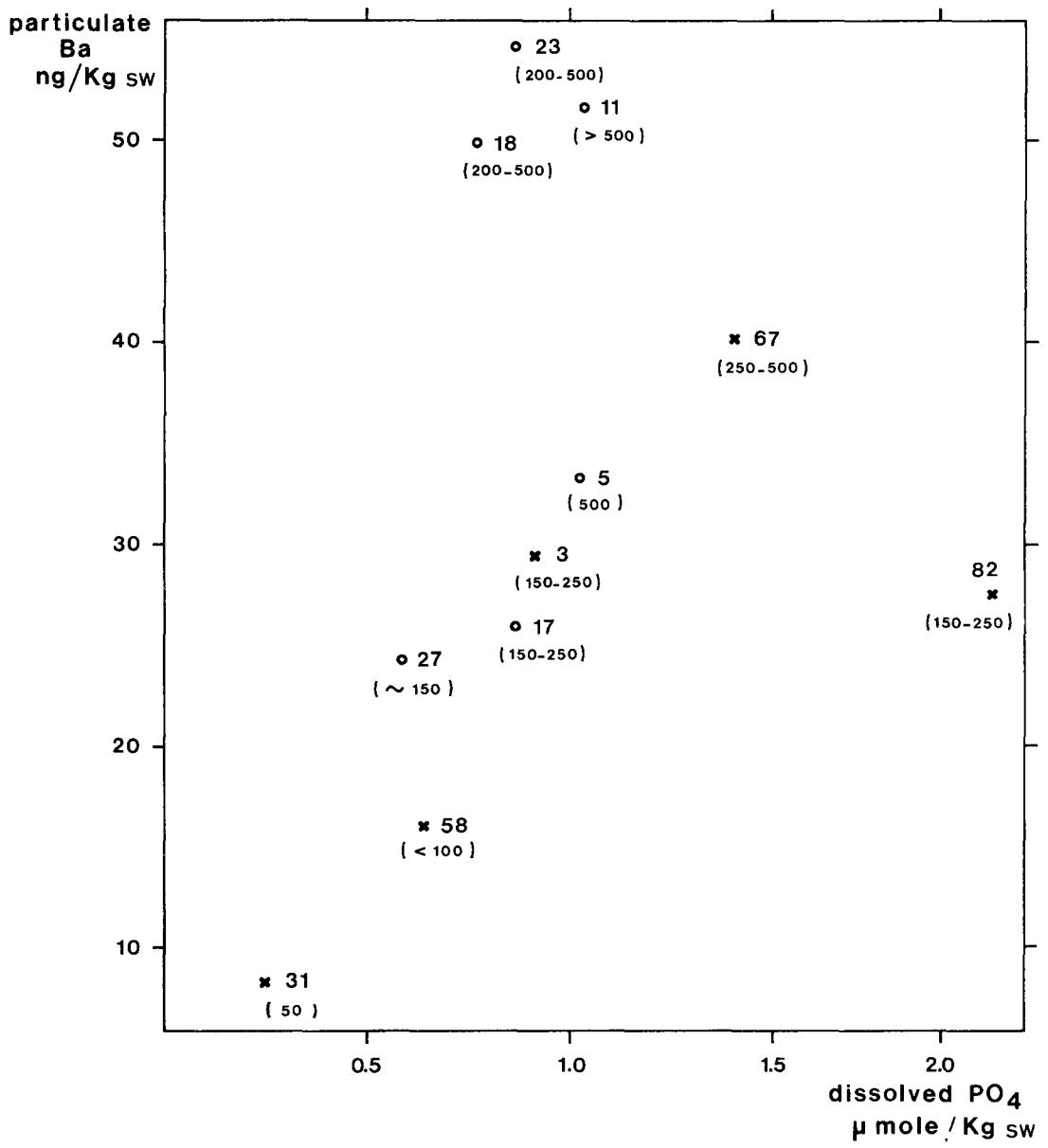

Fig. 10. Total Ba_p versus dissolved PO_4. The geometric mean Ba_p value (in ng/kg sw), observed between 150 and 1000 m is plotted against the geometric mean dissolved PO_4 value (in µmole/kg sw; GEOSECS ship-board data) for the same depth interval. Crosses refer to Ba_p measurements performed by INAA at the Centre des Faibles Radioactivités; open circles refer to measurements performed by INAA at the Woods Hole Oceanographical Institution by P. Brewer (GEOSECS shore-based data). Numbers refer to GEOSECS station numbers. Between brackets: values of organic carbon production rates (in mg C/m^2 day) from Koblentz-Mishke [44]; value for station 31 from Steeman-Nielsen [41].

the relative intensity of organic carbon production is considered.

Although this relationship between biological productivity and barite formation seems to hold, the maximum concentrations of barite are generally found just below the euphotic zone and the detailed pathway

between organic productivity and barite formation is not known. Two complementary pathways can be considered:

(1) Secretion of barite crystals by planktonic organisms and the release into the waters below the euphotic zone upon the death and disintegration of the organisms. Direct secretion of intracellular barite is known to occur in several species of the benthic protozoan *Xenophyophora* [45]. In surface waters only $SrSO_4$ (celestite)-secreting organisms, acantharid Radiolaria, have as yet been reported [46]. These, however, have a world-wide distribution and their spines can contain high levels of Ba (up to 5400 ppm) [25]. The central capsulum of certain species of collosphaerid Radiolaria contain rhombic crystals, identified as celestite and/or barite [47]. Finally, radiolarian-rich plankton has been observed to contain high Ba levels [31]. Such examples indicate that biological mediators can control the varying Ba/Sr molar ratios.

(2) Barite is formed during the decomposition of organic matter. Chow and Goldberg [1] proposed that decaying organic matter, rich in sulphate ions, could form a micro-environment in which $BaSO_4$ saturation is attained. We have in fact observed submicron sized, discrete barite crystals and aggregates of barite prisms inside low-density media, of organic composition (Fig. 8). These are likely to represent such micro-environments, with barite precipitated within them. Again, high productivity in the photic zone could thus induce a maximum of suspended barite in the subsurface waters.

4.5. The importance of suspended barite as a source of deep-sea dissolved Ba

Undersaturation with respect to $BaSO_4$ induces the dissolution of suspended barite in the water column.

4.5.1. Estimation of the dissolution rate of barite in the water column

We have looked systematically for traces of an etching or corrosion process affecting the barite particles. The morphological study (Fig. 6, section 3.2), revealed that suspended barite particles are nearly all affected, to different degrees, by dissolution. The edges of the euhedral particles are rounded (Fig. 6B, 1–3) and particles become ellipsoïdal and spherical (Fig. 6A, 1–3). Etching of the particles can occur (Fig. 6B, 3). Dissolution proceeds further in eroding the particles by means of a layer by layer alteration (Fig. 6C, 1, 2) or by a piercing of the particle (Fig. 6C, 3). The effect of dissolution is further indicated, at GEOSECS station 67, by the decrease in the numbers of barite particles with depth, as shown in Fig. 7.

If the dissolution rate constant and the particle size distribution of a substance in the water column are known, and if constancy of particle flux at any depth is assumed, the dissolution rate J can be calculated [48]:

$$J = \tfrac{1}{3}\rho k(\Sigma_i N_i D_i^2) \qquad (2)$$

where J = input of dissolved matter per unit volume and per unit time (= g/kg seawater yr); ρ = density of the particulate matter (= 4.5 g/cm^3 for barite); k = dissolution rate constant (cm/yr) (= $\epsilon\pi$ in equation 9 in Lal and Lerman [48]); N_i = particle number in size class i, per unit volume (number/kg seawater); and D_i = particle diameter; = class-midpoint of class i (cm).

The dissolution rate constant of barite was estimated from a comparative study of the size distributions of barite for successive samples in the water column. It was assumed that the sinking particles obey the Stokes settling and dissolution rate model proposed by Brun-Cottan [49] after an original model of Lal and Lerman [50]. The sample pairs for which it was possible to apply the model calculations are given in Table 7A, together with the derived dissolution rate constants (k). An order of magnitude difference exists between the lowest and the highest computed values of k. If barite dissolution is a surface-controlled process, as observed for other sulphate salts [51], the lower range of k values (0.05 and 0.1 μm/yr) is more compatible with the existing condition of low undersaturation for $BaSO_4$ in deep water, as discussed in Dehairs [29]. Therefore we have used an average k value of 0.075 μm/yr. Equation (2) was applied to all the barite size distributions of GEOSECS stations 67 and 3, and a depth-weighted J_{Ba} value was deduced. Table 7B shows the best estimate of J_{Ba} resulting from the dissolution of suspended barites identified in this study.

Since carriers of Ba other than barite exist, and

TABLE 7A

Dissolution rate constants of barite as deduced from a Stokes settling and dissolution rate model

Stations and considered sample pairs	Barite dissolution rate constant k (μm/yr)
67 (2574–2982 m)	0.05
3 (1975–2479 m)	0.1
3 (2989–3267 m)	0.4

TABLE 7B

Depth weighted J_{Ba} values for the GEOSECS stations 67 and 3, resulting from barite dissolution

Stations and considered depth interval	J_{Ba} (depth-weighted) for k = 0.075 μm/yr (μg/cm^2 yr)
67 (151–5304 m)	0.42
3 (105–3267 m)	0.36

since these are not conservative, we must also estimate the contribution of their dissolution to the overall J_{Ba} term.

4.5.2. The J_{Ba} flux resulting from the dissolution of SiO_2 and $CaCO_3$ skeletons

J_{CaCO_3} and the resulting J_{Ba}. We take $CaCO_3$ and particulate organic carbon (POC; = 1/2 × POM [52]) to represent, respectively, 6 and 30% by weight of TSM (Table 5) and consider a mean Atlantic Ocean organic C production rate of 7 mg/cm^2 yr [44]. By [$CaCO_3$]/[POC] × production rate of organic C, we obtain a mean $CaCO_3$ production rate of 1.4 mg/cm^2 yr. If an average $CaCO_3$ sedimentation rate of 0.34 mg/cm^2 yr is considered [43], it follows that about 80% (= 1.1 mg/cm^2 yr) of the $CaCO_3$ produced in the surface reservoir redissolves at depth. This J_{CaCO_3} agrees with data of Berger ([43]: 1.5 mg/cm^2 yr) and Li et al. ([53]: 1.7 mg/cm^2 yr).

Since the Ba content of $CaCO_3$ skeletons was assigned an upper limit of 200 ppm (section 4.3), the J_{Ba} resulting from the dissolution of carbonate debris is $\leqslant$0.22 μg/cm^2 yr.

J_{SiO_2} and the resulting J_{Ba}. We take silica to represent 10%, and POC 30%, of the weight of TSM (Table 5). By [SiO_2]/[POC] × production rate of organic C (with POC and C production rate values as given above), it ensues that biogenic silica production is 2.3 mg/cm^2 yr. This value is higher than that computed by Berger ([43]: 1.3 mg/cm^2 yr) but is in agreement with the value of Harriss ([54]: 2.1 mg/cm^2 yr). The dissolution of opal at depth can amount to 97% of the quantity produced in surface waters [55]. With silica tests containing 120 ppm of Ba (section 4.3), their dissolution results in a J_{Ba} of 0.28 μg/cm^2 yr.

Summarizing, the overall J_{Ba} (0.9 μg/cm^2 yr) is composed of J_{Ba}-barite (0.4 μg/cm^2 yr); J_{Ba}-SiO_2 (0.3 μg/cm^2 yr); J_{Ba}-$CaCO_3$ (0.2 μg/cm^2 yr). This overall J_{Ba} value is in closer agreement with that calculated using a vertical advection diffusion model in the Pacific Ocean (0.7 μg/cm^2 yr) [56], than with that deduced by box-model calculations (3.5 μg/cm^2 yr) [3,4].

We agree with the conclusions of Chan et al. [2] that the distribution of dissolved Ba is governed by the dissolution of a slowly dissolving phase. Our data show that each of the phases suggested by Chan et al. (barite-carbonate-silica) is of about equal importance.

4.6. The role of suspended barite in the accumulation of barium in the sediments

Church [7] showed that in areas of rapid carbonate deposition, the barium accumulation associated with carbonate, clay, and organic matter, was sufficient to account for the observed levels of barite in the sediments. The biogenic particulate matter accumulating in the sediments is likely to have been conveyed by fast-settling fecal material [26,35,57, 58, 62]. Due to its high settling velocity, it is likely that most of this fecal material arrives intact at the sediments. The associated flux of barium was calculated by considering POM, SiO_2 and $CaCO_3$ to contain 60, 120 and 200 ppm of Ba respectively (Table 6), and using the Bishop et al. [62,26] flux data for these main components, obtained for the Equatorial Atlantic [26] and the Cape Basin [62]. The resulting fecal matter flux of Ba amounts to between 0.03 and 0.5 μg/cm^2 yr.

It is likely that this flux is supplemented by a conservative flux of suspended barite. The upper limit of

this flux can be computed from our size distribution data as given in Fig. 7, assuming Stokes settling law, by solving:

$$B = \sum_i m_i v_i \qquad (3)$$

where B = vertical flux of barite (μg Ba/cm^2 yr); m_i = Ba concentration (μg/cm^3) of barite in size class i; and v_i = Stokes settling velocity of the barites of size i (cm/yr).

As applied to the deep-sea samples of the stations 67 and 3, equation (3) gives: station 67, 5304 m: B = 0.4 μg Ba/cm^2 yr; station 3, 3267 m: B = 0.4 μg Ba/cm^2 yr. Assuming that such fluxes reach the sediments, it appears that settling of suspended barite can at least be as important as Ba associated with the flux of fecal material. The total Ba flux (fecal material + barite) amounts to between 0.43 and 0.9 μg Ba/cm^2 yr, which is in agreement with the sedimentary Ba accumulation rate of Turekian ([15,59]: 0.5–1.0 μg/cm^2 yr).

The total flux of particulate barium to the sediments computed here appears to balance the amount of dissolved Ba introduced to the oceans by river discharge (0.6 μg/cm^2 yr) [3,4,56]. Adding to this the barium reintroduced to the dissolved phase (0.9 μg/cm^2 yr), the rate of particulate Ba production (A) should amount to about 1.5 μg/cm^2 yr to maintain steady state. A rough calculation, assuming that all of the barium in the annual production of that POM which is not lost to the sediments (0.8 μg Ba/cm^2 yr) is converted to barite, and adding the annual incorpo-

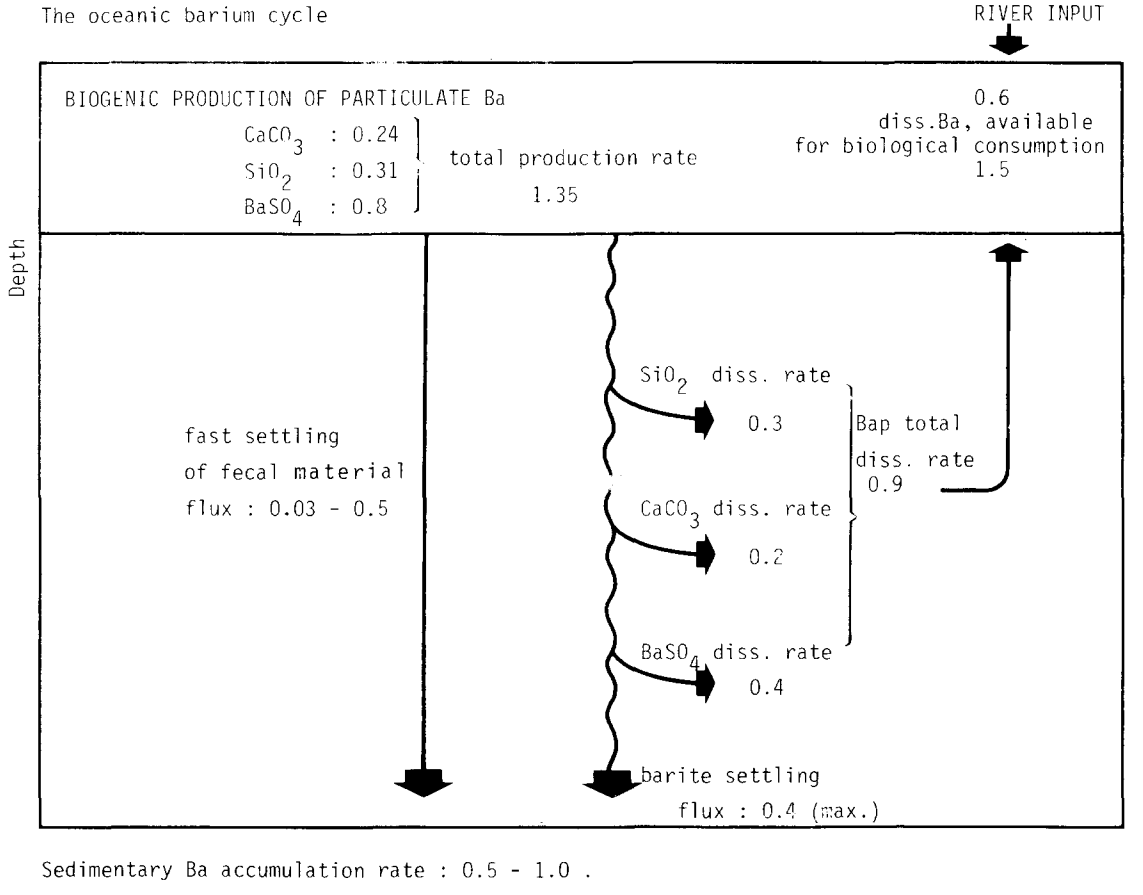

Fig. 11. Numerical values for the components of the oceanic barium cycle. All values in μg Ba/cm^2 yr. Arrows indicate the direction of the fluxes.

ration of barium into skeletal material (0.55 $\mu g/cm^2$ yr), gives a figure (B) of 1.35 $\mu g/cm^2$ yr. The agreement between A and B affirms the importance of biological activity and the recycling of barium in the water column. Fig. 11 summarizes the gross budget of barium in the ocean, as based on our data.

5. Summary and conclusions

Discrete micron-sized barite particles are present in suspended matter everywhere in the World Ocean.

A combination, in the same suspended matter samples, of quantitative analyses of the total barium content and quantitative assessments of the numbers and mass of Ba of the discrete barite particles, show that barite is the main carrier of Ba in intermediate and deep ocean waters. In surface waters organic and skeletal debris comprise a significant portion of the total particulate barium. In bottom waters resuspended aluminosilicates can dominate over other forms of non-barite particulate barium.

The repartition of Ba between organic, skeletal and barite phases indicates that barite is first introduced in surface waters by biological processes, and that such processes subsequently lead to barite maxima in intermediate waters.

The link between barite production and biological activity is emphasized by a positive relationship between the particulate barium content in surface waters and biological productivity. The kinds of processes which may be responsible are: direct secretion of barite within planktonic organisms, and precipitation within the micro-environments of decaying organic debris.

Dissolution of barite in the deep ocean proceeds at a rate of 0.4 μg Ba/cm^2 yr. A supplementary flux, which is of the same magnitude, is the flux of dissolved barium resulting from the dissolution of SiO_2 and $CaCO_3$ tests.

The residual flux of barite reaching the sea floor can account for half of the total sedimentation rate of barium in regions of high productivity.

The budget for barium in the ocean, as derived from our data, affirms the importance of biological activity. This budget is to a large degree self-sustained by the input to the water column of dissolved barium resulting from the dissolution of suspended barite and other biogenic particles.

Acknowledgements

This work could not have been achieved without the assistance of C.E. Lambert for the neutron activation analyses, of J.C. Brun-Cottan for the interpretation of the size distribution data, of J. Klossa in obtaining the electron diffractograms and of C. Jehanno for the scanning electron microscope and electron microprobe analyses. We are very grateful to T. Church, P. Biscaye, P. Buat-Menard, D. Spencer, P. Brewer, R. Wollast and A. Herbosch for their fruitful discussions and suggestions. We also wish to thank the three anonymous reviewers, as well as D. Losman and N. Silverberg for the suggested improvements of the initial manuscript. We are indebted to the GEOSECS Operations Group and especially to A. Bainbridge for providing the suspended matter samples, and to the Laboratoire d'Analyses par Activation "Pierre Sue", CNRS-CEA, Centre d'Etudes Nucléaires, Saclay, France, for providing the facilities for neutron activation analysis. This work was supported by a GEOSECS-NSF grant, through subcontracts with the Woods Hole Oceanographical Institution (1972–1973), Columbia University (1974–1975), and the University of Miami (1976–1977).

References

1 T.J. Chow and E.D. Goldberg, On the marine geochemistry of barium, Geochim. Cosmochim. Acta 20 (1960) 192.
2 L.H. Chan, D. Drummond, J.M. Edmond and B. Grant, On the barium data from the Atlantic GEOSECS expedition, Deep-Sea Res. 24 (1977) 613.
3 K. Wolgemuth and W.S. Broecker, Barium in sea water, Earth Planet. Sci. Lett. 8 (1970) 372.
4 Y.H. Li, T.L. Ku, G.G. Mathieu and K. Wolgemuth, Barium in the Antarctic Ocean and implications regarding the marine geochemistry of Ba and ^{226}Ra, Earth Planet. Sci. Lett. 19 (1973) 352.
5 E. Goldberg and G. Arrhenius, Chemistry of pelagic sediments, Geochim. Cosmochim. Acta 33 (1969) 894.
6 K.K. Turekian and E.H. Tausch, Barium in deep-sea sediments of the Atlantic Ocean, Nature 201 (1964) 696.
7 T.M. Church, Marine barite, Ph.D. Thesis, University of California (1970).
8 J.S. Hanor, Rates of barium accumulation in the Equatorial Pacific, Geol. Soc. Am., Abstr. Progr. 4 (1972) 526.
9 K. Boström, O. Joensuu, C. Moore, B. Boström, M. Dalziel and A. Horowitz, Geochemistry of barium in pelagic sediments, Lithos 6 (1973) 159.

10 T.L. Ku, Y.H. Li, G.G. Mathieu and H.K. Wong, Radium in the Indian-Antarctic Ocean south of Australia, J. Geophys. Res. 75 (1970) 5286.
11 J.M. Edmond, Comments on the paper by T.L. Ku, Y.H. Li, G.G. Mathieu and H.K. Wong, "Radium in the Indian-Antarctic Ocean south of Australia", J. Geophys. Res. 75 (1970) 6878.
12 M.P. Bacon and J.M. Edmond, Barium at GEOSECS III in the Southeast Pacific, Earth Planet. Sci. Lett. 16 (1972) 66.
13 M. Brongersma-Sanders, Barium in pelagic sediments and in diatoms, K. Ned. Akad. Wet. Proc. B70 (1966) 93.
14 Z.A. Vinogradova and V.V. Koval'skiy, Elemental composition of the Black Sea plankton, Dokl. Akad. Nauk USSR, Earth Sci. Sect. 147 (1962) 217.
15 K.K. Turekian, Deep-sea deposition of barium, cobalt and silver, Geochim. Cosmochim. Acta 32 (1968) 603.
16 F.E. Schulze and H. Thierfelder, Bariumsulfat in Meerestieren (*Xenophyophora*, F.E. Sch.), Sitzungsber. Ges. Naturforsch. Freunde Berlin (1905) 2.
17 G. Arrhenius and E. Bonatti, Neptunism and vulcanism in the ocean, in: Progress in Oceanography, 3, F. Koczy, ed. (1965) 7.
18 C. Darcourt, Etude des matières en suspension dans les eaux profondes Atlantiques: teneurs en éléments traces mesurées par activation neutronique, comparaisons avec le sédiment, Thèse Doct. 3è Cycle, Université de Paris 6 (1973).
19 R. Chesselet, J. Jedwab, C. Darcourt and F. Dehairs, Barite as discrete suspended particles in the Atlantic Ocean, EOS, Am. Geophys. Union 57 (1976) 255 (abstract).
20 D.W. Spencer, P.G. Brewer, R. Chesselet, P.E. Biscaye and J. Jedwab, Dissolution and composition of suspended matter in the Atlantic Ocean, Abstr. IUGG Assem., Grenoble (1975).
21 P.G. Brewer, D.W. Spencer, P.E. Biscaye, A. Hanley, P.L. Sachs, C.L. Smith, S. Kadar and J. Fredericks, The distribution of particulate matter in the Atlantic Ocean, Earth Planet. Sci. Lett. 32 (1976) 393.
22 J. Klossa, Contribution à l'étude de la matière particulaire par une méthode d'analyses ponctuelles combinées, Thèse Doct. 3è Cycle, Université de Paris 6 (1977).
23 T. Allen, Particle Size Measurement (Chapman and Hall, London, 1968).
24 C.E. Lambert, Contribution à l'étude du fer et de l'aluminium particulaires dans l'océan, Thèse de diplôme d'Etudes supérieures, Université de Picardie (1979).
25 G. Arrhenius, Pelagic sediments, in: The Sea, 3, M.N. Hill, ed. (Wiley-Interscience, New York, N.Y., 1963) 655.
26 J.K. Bishop, J.M. Edmond, D.R. Ketten, M.P. Bacon and W.B. Silker, The chemistry, biology and vertical flux of particulate matter from the upper 400 m of the Equatorial Atlantic Ocean, Deep-Sea Res. 24 (1977) 511.
27 T.M. Church and K. Wolgemuth, Marine barite saturation, Earth Planet. Sci. Lett. 15 (1972) 35.
28 O. Aubey, Contribution à l'étude de la dissolution des particules de carbonate de calcium dans les eaux profondes océaniques, Thèse 3è Cycle, Université de Paris 6 (1976).
29 F. Dehairs, Discrete suspended particles of barite and the barium cycle in the open ocean, Doctoral Thesis in Science, Vrije Universiteit, Brussels (1979).
30 H. Bernat, T. Church and C.J. Allègre, Barium and strontium concentrations in Pacific and Mediterranean seawater profiles by direct isotope dilution mass spectrometry, Earth Planet. Sci. Lett. 16 (1972) 75.
31 J. Martin and G.A. Knauer, The chemical composition of plankton, Geochim. Cosmochim. Acta 37 (1973) 1639.
32 J.P. Riley and I. Roth, The distribution of trace elements in some species of phytoplankton grown in culture, J. Mar. Biol. Assoc. U.K. 51 (1971) 63.
33 C. Copin-Montegut and G. Copin-Montegut, Chemical analysis of suspended particulate matter collected in the northeast Atlantic, Deep-Sea Res. 19 (1972) 445.
34 C. Copin-Montegut and G. Copin-Montegut, The chemistry of particulate organic matter from the south Indian and Antarctic Ocean, Deep-Sea Res. 25 (1978) 911.
35 S. Krishnaswami, D. Lal and B.L.K. Somayajulu, Investigations of gram quantities of Atlantic and Pacific surface particulates, Earth Planet. Sci. Lett. 32 (1976) 403.
36 R. Chesselet, D.W. Spencer and P.E. Biscaye, Element transport by particles: the aluminium, manganese, iron system in Atlantic suspended matter, in: Book of Abstracts, Geochemistry and Ocean Mixing Symposium, Joint Oceanographic Assembly, Edinburgh 1976 (F.A.O., Rome, 1976).
37 P. Buat-Menard and R. Chesselet, Variable influence of the atmospheric flux on the trace metal chemistry of oceanic suspended matter, Earth Planet. Sci. Lett. 42 (1979) 399.
38 K.K. Turekian and K.H. Wedepohl, Distribution of the elements in some major units of the Earth's crust, Geol. Soc. Am. Bull. 72 (1961) 175.
39 J.S. Hanor, Barite saturation in sea water, Geochim. Cosmochim. Acta 33 (1969) 894.
40 T.M. Church, Barium sulfate solubility in seawater (submitted to Earth Planet. Sci. Lett.).
41 E. Steeman-Nielsen, On organic production in the oceans, J. Cons., Int. Explor. Mer 19 (1954) 309.
42 J.L. Reid, On circulation, phosphate-phosphorus content, and zooplankton volumes in the upper part of the Pacific Ocean, Limnol. Oceanogr. 7 (1962) 287.
43 W.H. Berger, Biogenous deep-sea sediments; fractionation by deep-sea circulation, Geol. Soc. Am. Bull. 81 (1970) 1385.
44 O.J. Koblentz-Mishke, V.V. Volkovinsky and J.G. Kabanova, Plankton primary production of the world ocean, in: Scientific Exploration of the South Pacific, W.S. Wooster, ed. (U.S. National Academy of Science, Washington, D.C., 1970) 183.
45 O.S. Tendal, A monograph of the Xenophyophoria, Galathea Rep. 12 (1972) 8.
46 E.M. Botazzi and B. Schreiber, *Acantharia* in the Atlantic Ocean, their abundance and preservation, Limnol. Oceanogr. 16 (1971) 677.
47 E. Haeckel, Radiolarien (Rhizopoda Radiolaria), Eine Monographie (G. Reimer Verlag, Berlin, 1862).

48 D. Lal and A. Lerman, Dissolution and behaviour of particulate biogenic matter in the ocean: some theoretical considerations, J. Geophys. Res. 78 (1973) 7100.
49 J.C. Brun-Cottan, Stokes settling and dissolution rate model for marine particles as a function of size distribution, J. Geophys. Res. 81 (1976) 1601.
50 D. Lal and A. Lerman, Size spectra of biogenic particles in ocean water and sediments, J. Geophys. Res. 80 (1975) 423.
51 J.R. Campbell and G.H. Nancollas, The crystallization and dissolution of strontium sulfate in aqueous solution, J. Phys. Chem. 73 (1969) 1735.
52 J.D.H. Strickland, Production of organic matter in the primary stages of the marine food chain, in: Chemical Oceanography, 2, J.P. Riley and G. Skirrow, eds. (Academic Press, New York, N.Y., 1965) 477.
53 Y.H. Li, T. Takahashi and W.S. Broecker, Degree of saturation of $CaCO_3$ in the oceans, J. Geophys. Res. 74 (1969) 5507.
54 R.C. Harriss, Biological buffering of oceanic silica, Nature 212 (1966) 275.
55 R. Wollast, The silica problem, in: The Sea, 5, E.D. Goldberg, ed. (Wiley, New York, N.Y., 1974) 659.
56 L.H. Chan, J.M. Edmond, R.F. Stallard, W.S. Broecker, Y.C. Chung, R.F. Weiss and T.L. Ku, Radium and Barium at GEOSECS stations in the Atlantic and Pacific, Earth Planet. Sci. Lett. 32 (1976) 258.
57 I.N. McCave, Vertical flux of particles in the Ocean, Deep-Sea Res. 22 (1975) 491.
58 H.J. Schrader, Fecal pellets: role in sedimentation of pelagic diatoms, Science 174 (1971) 55.
59 K.K. Turekian and D.G. Johnson, The barium distribution in seawater, Geochim. Cosmochim. Acta 30 (1966) 1153.
60 C.E. Lambert, C. Jehanno, J.C. Brun-Cottan, N. Silverberg and R. Chesselet, Size distribution of suspended aluminosilicates in deep South Atlantic waters (submitted to Deep-Sea Res.).
61 P.E. Biscaye and S.L. Eittreim, Suspended particulate loads and transports in the nepheloid layer of the abyssal Atlantic Ocean, Mar. Geol. 23 (1977) 155.
62 J.K.B. Bishop, D.R. Ketten and J.M. Edmond, The chemistry, biology and vertical flux of particulate matter from the upper 400 m of the Cape Basin in the southeast Atlantic Ocean, Deep-Sea Res. 25 (1979) 1121.